

AutoCost: Evolving Intrinsic Cost for Zero-violation Reinforcement Learning

Tairan He, Weiye Zhao, Changliu Liu

Robotics Institute, Carnegie Mellon University
{tairanh, weiyezha, cliu6}@andrew.cmu.edu

Abstract

Safety is a critical hurdle that limits the application of deep reinforcement learning (RL) to real-world control tasks. To this end, constrained reinforcement learning leverages cost functions to improve safety in constrained Markov decision processes. However, such constrained RL methods fail to achieve zero violation even when the cost limit is zero. This paper analyzes the reason for such failure, which suggests that a proper cost function plays an important role in constrained RL. Inspired by the analysis, we propose AutoCost, a simple yet effective framework that automatically searches for cost functions that help constrained RL to achieve zero-violation performance. We validate the proposed method and the searched cost function on the safe RL benchmark Safety Gym. We compare the performance of augmented agents that use our cost function to provide additive intrinsic costs with baseline agents that use the same policy learners but with only extrinsic costs. Results show that the converged policies with intrinsic costs in all environments achieve zero constraint violation and comparable performance with baselines.

1 Introduction

Reinforcement learning (RL) has achieved remarkable progress in board games (Mnih et al. 2015), card games (Brown and Sandholm 2018) and video games (Vinyals et al. 2019). Despite its impressive success so far, the lack of safety guarantees limits the application of RL to real-world physical tasks like robotics. This is particularly concerning for safety-critical scenarios such as robot-human collaboration or healthcare where unsafe controls may lead to fatal consequences.

Many safe RL methods leverage cost functions defined in constrained Markov decision process (CMDP) (Altman 1999) to formulate safety. Recent approaches usually adopt *indicator cost functions* where a positive signal deems a state as unsafe and zero deems a state safe. However, under such a design of cost functions, state-of-the-art safe RL methods still fail to achieve zero violation even with sufficiently enough interactions with the environment (Ma et al. 2021). For example, Figure 1 illustrates the average episodic extrinsic cost (i.e., constraint violations in CMDP) of two safe

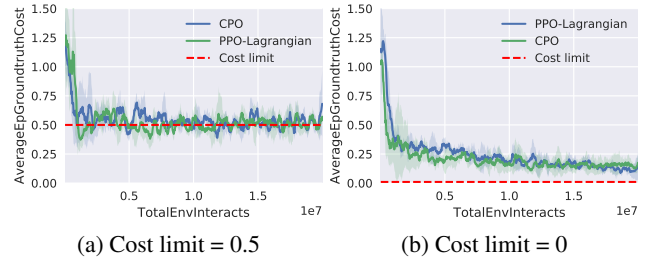


Figure 1: Average episodic extrinsic cost of safe RL baselines with different limit. CPO and PPO-Lagrangian both fail to achieve zero violation even with a zero cost limit

RL baselines (Achiam et al. 2017; Chow et al. 2017) in the commonly used safe RL benchmark Safety Gym.

Note that though the average extrinsic cost reduces to 0.5 when the cost limit is set as 0.5, both safe RL baselines with zero cost limit fail to obtain a zero-violation policy even after convergence. Nevertheless, in safety-critical applications, reducing the number of safety violations may not be sufficient since one violation may lead to unacceptable catastrophes. How to eliminate all violations and achieve zero violation remains a challenge for RL.

To break this barrier, in this paper, we conduct an empirical analysis on why safe RL methods fail to achieve zero violation. We find that the reason is closely related to the design of cost functions, where a proper cost function could drive the converged safe RL policies to achieve zero violation. However, designing cost functions has the same issues as designing reward functions (Hong et al. 2018; Faust, Francis, and Mehta 2019), which requires extensive human efforts. To this end, instead of handcrafting a cost function with expert knowledge, we propose AutoCost which automatically searches for proper cost functions with the aim of obtaining a zero-violation policy, relieving researchers from such tedious work. AutoCost formulates the problem as a bi-level optimization where we try to find the best intrinsic cost function, which, to the most extent, helps train a zero-violation RL agent. Specifically, AutoCost utilizes an evolutionary strategy to search the parameters of cost function.

We apply the evolutionary intrinsic cost search to an environment in Safety Gym (Ray, Achiam, and Amodei 2019), over two safe RL algorithms: Constrained Policy Optimization (CPO) (Achiam et al. 2017) and Lagrangian Proximal

Policy Optimization (PPO-Lagrangian) (Chow et al. 2017). We optimize the parameters of intrinsic cost functions over two objectives: *cost rate* and *reward performance*. The results show that augmented agents that use the searched cost function to provide additive intrinsic costs achieve zero violation under different settings including (i) different control tasks; (ii) different robots; (iii) different types of obstacles. We further analyze why the searched intrinsic cost function boosts the safety of RL agents, revealing that some vital properties of cost functions like local awareness and dense signals are beneficial to safe RL methods. The main contribution of this paper are listed as follows:

- We find that different safe RL algorithms react differently to cost functions. We analyze the failure of current safe RL algorithms and point out that a proper cost function is the key to zero-violation RL policies.
- To the best of our knowledge, we are the first to propose automated searching for cost function to achieve zero-violation safety performance.
- We evaluate the searched cost function with different safe RL algorithms on state-of-the-art safe RL benchmarks. Results show that the converged policies with intrinsic costs in all environments achieve zero constraint violation and comparable performance with baselines.

2 Related Work

2.1 Safe RL

The safe RL algorithms can be divided into three categories.

- **Lagrangian method:** Lagrangian multiplier (Boyd, Boyd, and Vandenberghe 2004) provides a regularization term to penalize objectives with constraint violations. Previous work (Chow et al. 2017) derives a formula to compute the gradient of the Lagrangian function in CMDP. Some safe RL works (Liang, Que, and Modiano 2018; Tessler, Mankowitz, and Mannor 2018) solve a primal-dual optimization problem to satisfy constraints. Another work (Stooke, Achiam, and Abbeel 2020) leverages derivatives of the constraint function and PID Lagrangian methods to reduce violations during agent learning. More recent work (Chen, Dong, and Wang 2021) gives an analysis on the convergence rate for sampling-based primal-dual Lagrangian optimization.
- **Direct policy optimization methods:** Though Lagrangian methods are easy to transfer to the setting of safe RL, the resulted policy was only safe asymptotically and lacks safety guarantees during each training iteration (Chow et al. 2018). Therefore, many works propose to derive surrogate algorithms with direct policy optimization. One representative method is constrained policy optimization (Achiam et al. 2017) which leverages the trust region of constraints for policy updates. Another work (El Chamie, Yu, and Açıkmeşe 2016) proposes a conservative stepwise surrogate constraint and leverages linear programming to generate feasible safe policies. FOCOPS (Zhang, Vuong, and Ross 2020) proposes a convex approximation to replace surrogate functions with first-order Taylor expansion.

- **Safeguard-based methods:** Another line of safe RL works add a safeguard upon the policy network, projecting unsafe actions to safe actions. Some works (Srinivasan et al. 2020; Bharadhwaj et al. 2020) leverage a safety critic to detect unsafe conditions and use such a critic to choose the safe action. Safety layer (Dalal et al. 2018) solves a QP problem to safeguard unsafe actions with learned dynamics, but it is limited to linear cost functions. ISSA (Zhao, He, and Liu 2021) proposes an efficient sampling algorithm for safe actions and guarantees zero violation during agent learning, but it also requires a perfect dynamics model for a one-step prediction. ShieldNN (Ferlez et al. 2020) designs a safety filter neural network with safety guarantees specifically for the kinematic bicycle model (KBM) (Kong et al. 2015), which limits the generalization ability to other dynamics.

Besides different methodology, the types of safety considered by these safe RL algorithms are also different. Most Lagrangian and direct policy optimization methods consider safety as the cost expectation of trajectories being lower than a cost limit (i.e., *safety in expectation*), while safeguard-based methods consider *state-wise safety*. However, safeguard-based methods usually require either the dynamics model or prior knowledge as discussed above, which is unrealistic in practice. Our work aims to boost general safe RL algorithms (i.e., the first two categories) to achieve safety in expectation but with a zero cost limit. Note that strictly satisfying a zero cost limit in expectation is actually equivalent to state-wise safety. So our framework is a vital step that bridges *safety in expectation* and *state-wise safety*.

2.2 Certificate of Safety

Besides the cost function of CMDP used in safe RL, there are many different certificates (Wei and Liu 2019) to measure safety in the safe control community including (i) potential function; (ii) safety index; (iii) control barrier function. Representative methods include potential field method (Khatib 1986), sliding mode algorithm (Gracia, Garelli, and Sala 2013), barrier function method (Ames, Grizzle, and Tabuada 2014), and safe set algorithm (Liu and Tomizuka 2014). However, designing such safety certificate functions is difficult and requires great human efforts to find appropriate parameters and functional forms (Dawson, Gao, and Fan 2022; Zhao, He, and Liu 2021). Some automated synthesis techniques for safety certificates are either computationally expensive (Giesl and Hafstein 2015) or limited to specific dynamics (Ahmadi and Majumdar 2016). Recently, many works (Chang, Roohi, and Gao 2019; Qin et al. 2021; Dawson et al. 2022) leverage neural networks to learn such safety certificates. But such methods require prior signals (e.g., safe and unsafe regions) for supervised learning, whereas our framework searches for proper intrinsic cost functions automatically with the goal of zero violation.

2.3 Automating RL

How to automate RL has been an active topic recently. Some works leverage techniques from the AutoML community to automate the process of hyper-parameters searching (Paul,

Kurin, and Whiteson 2019; Zahavy et al. 2020; Xu et al. 2020) and architectures searching (Runge et al. 2018; Franke et al. 2020) for RL. Besides, designing a reward function that encourages the desired behaviors while still being learnable for RL is difficult (Dewey 2014). To this end, AutoRL (Faust, Francis, and Mehta 2019) proposes to automatically search for better reward functions in an evolutionary manner. Another work (Veeriah et al. 2019) proposes to discover more helpful value/reward functions using meta gradients. LIRPG (Zheng, Oh, and Singh 2018) proposes an algorithm for learning intrinsic rewards for RL. To the best of our knowledge, we are the first to automate the process of designing cost functions for zero-violation safe RL.

3 Problem Formulation and Background

3.1 Constrained Markov Decision Process

We consider constrained Markov decision process (CMDP) defined as the tuple $(\mathcal{S}, \mathcal{A}, P, \mathcal{R}, \mathcal{C}, \rho_0, \gamma)$ with following components: states $s \in \mathcal{S}$, actions $a \in \mathcal{A}$, P is the distribution of state transition where $P = P(s_{t+1}|s_t, a_t)$, $\rho_0 : \mathcal{S} \rightarrow [0, 1]$ is the initial state distribution, $\gamma \in [0, 1]$ is the discounted factor. The agent holds its policy $\pi(a|s) : \mathcal{S} \times \mathcal{A} \rightarrow [0, 1]$ to make decisions and receive rewards defined as $r : \mathcal{S} \rightarrow \mathbb{R}$ and cost defined as $c : \mathcal{S} \rightarrow \mathbb{R}$. To distinguish between the cost function defined in the CMDP and other additive cost functions, we denote the original cost function in the CMDP as the *extrinsic cost* as $c^{ex} : \mathcal{S} \rightarrow \mathbb{R}$, and we denote *intrinsic cost* parameterized by θ as $c_\theta^{in} : \mathcal{S} \rightarrow \mathbb{R}$.

In RL, we aim to select a policy π which maximizes the discounted cumulative rewards $\mathcal{R}^\pi := \mathbb{E}_{\tau \sim \pi} [\sum_{t=0}^{\infty} \gamma^t r_t]$. Meanwhile, the extrinsic cost function c^{ex} in CMDP defines the cost return as $J_{c^{ex}}^\pi := \mathbb{E}_{\tau \sim \pi} [\sum_{t=0}^{\infty} \gamma^t c_t^{ex}]$. Based on these two definitions, the feasible policies $\Pi_{c^{ex}}$ and optimal policies π^* in CMDP are defined as:

$$\Pi_{c^{ex}} := \{\pi \in \Pi : J_{c^{ex}}^\pi \leq d\}, \pi^* = \arg \max_{\pi \in \Pi_{c^{ex}}} \mathcal{R}^\pi \quad (1)$$

The goal of constrained RL algorithms is:

$$\max_{\pi \in \Pi} \mathcal{R}^\pi \quad \text{s.t.} \quad J_{c^{ex}}^\pi \leq d \quad (2)$$

3.2 Proximal Policy Optimization

Proximal policy optimization (PPO) (Schulman et al. 2017) is an on-policy policy gradient algorithm. PPO proposes a surrogate objective that attains the data efficiency and reliable performance of TRPO (Schulman et al. 2015) while using only first-order optimization:

$$\pi_{k+1} = \arg \min_{\pi \in \Pi} \mathbb{E}_{\tau \sim \pi_k} \min \left(\frac{\pi(a|s)}{\pi_k(a|s)} A_r^{\pi_k}(s, a), \text{clip}\left(\frac{\pi(a|s)}{\pi_k(a|s)}, 1 - \epsilon, 1 + \epsilon\right) A_r^{\pi_k}(s, a) \right), \quad (3)$$

where $A_r^{\pi_k}$ is the advantage function of reward with respect to π_k and ϵ is a (small) hyper-parameter determining how far away the new policy π_{k+1} is allowed to go from the old π_k .

3.3 Lagrangian Methods

Lagrangian methods (Boyd, Boyd, and Vandenberghe 2004) use adaptive coefficients to enforce constraints in optimization with $f(\omega)$ the objective and $g(\omega) \leq 0$ the constraint:

$$\max_{\omega} \min_{\lambda \geq 0} \mathcal{L}(\omega, \lambda) = f(\omega) - \lambda g(\omega) \quad (4)$$

Similarly, Lagrangian safe RL (Chow et al. 2017) adopt such an iterative learning scheme to solve Equation (2) as:

$$\max_{\pi} \min_{\lambda \geq 0} \mathcal{L}(\pi, \lambda) = \mathcal{R}^\pi - \lambda (J_{c^{ex}}^\pi - d) \quad (5)$$

In the implementation, Lagrangian safe RL methods iteratively take gradient ascent steps with respect to π and gradient descent with respect to λ .

3.4 Constrained Policy Optimization

CPO (Achiam et al. 2017) analytically solves trust region optimization problems at each policy update to enforce constraints throughout training:

$$\begin{aligned} \pi_{k+1} &= \arg \max_{\pi \in \Pi} \mathbb{E}_{s \sim \pi_k, a \sim \pi} [A_r^{\pi_k}(s, a)] \\ \text{s.t.} \quad & J_{c^{ex}}^{\pi_k} + \frac{1}{1 - \gamma} \mathbb{E}_{s \sim \pi_k, a \sim \pi} [A_{c^{ex}}^{\pi_k}(s, a)] \leq d \\ & \hat{D}(\pi || \pi_k) \leq \delta, \end{aligned} \quad (6)$$

where $A_r^{\pi_k}$ and $A_{c^{ex}}^{\pi_k}$ are advantage functions of reward and extrinsic cost functions with respect to π_k .

4 Empirical Observation and Analysis

In this section, we begin with empirical observations that motivate the core idea of our method to design cost functions in order to achieve zero violation. Generally, we aim to investigate why safe RL methods fail to achieve zero violation as shown in Figure 1. We come up with two hypotheses and verify them in the following subsections.

4.1 More Conservative Cost Limit

Inspired by Figure 1, we find that safe RL does not strictly meet the requirements of the cost limit and oscillates around the threshold. To further eliminate violations, we attempt a more conservative cost limit (i.e., a negative cost limit). The results are shown in Figure 2, where CPO achieves near zero violation with the cost limit of -0.1 and achieves zero violation with the cost limit of -1.0 , but with significant performance drops. On the contrary, negative cost limits do not affect PPO-Lagrangian differently compared with the zero cost limit. The reason behind the difference is that a negative cost limit makes CPO update policies in the most conservative way (i.e., only considering constraints). As for Lagrangian methods, a negative cost limit just applies the relatively same penalty on objectives at each policy update. We conclude that tuning the cost limit is possible to help CPO to achieve zero violation (with significant performance drops) but can not help Lagrangian methods. To find a more general method to drive safe RL agents to achieve zero violation, we turn to the design of cost functions.

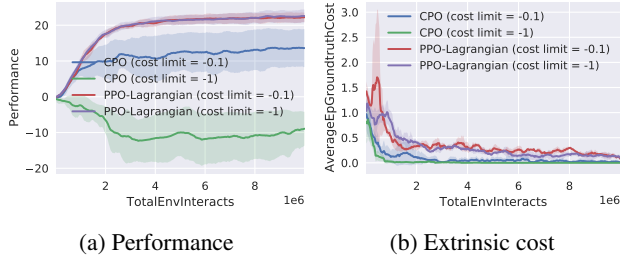


Figure 2: Average episodic reward and cost of safe RL baselines with negative cost limit.

4.2 Denser Cost Function

The sparsity (costs only obtained on constraint violation) of indicator cost functions has the same issue of sparse reward functions (Andrychowicz et al. 2017). Similarly, we apply a commonly used dense reward design to cost functions:

$$c(s_t) = \max(d(s_{t-1}) - d(s_t), 0), \quad (7)$$

where $d(\cdot)$ denotes the distance from RL agent to the closet constraint. Note that this dense cost function is very conservative because it assigns positive costs to any step making the RL agent closer to constraints. We train CPO and PPO-Lagrangian under the denser cost function. The results are shown in Figure 3, where we find that the dense cost function is detrimental to RL performance of CPO though it helps CPO quickly converges to a zero-violation policy. On the other hand, PPO-Lagrangian converges to a near zero-violation policy in the end with satisfying reward performance. We point out that safe RL algorithms react differently under the same cost function due to different algorithmic designs. One cost function may be suitable for a specific algorithm but may be detrimental to another algorithm. How to find a more generalizable cost function for different safe RL algorithms remains a challenge. We also try more hand-designed cost functions (details are given in Appendix A.1), but none is good enough to achieve both zero violation and satisfying reward performance, indicating the difficulty of manually designing cost functions.

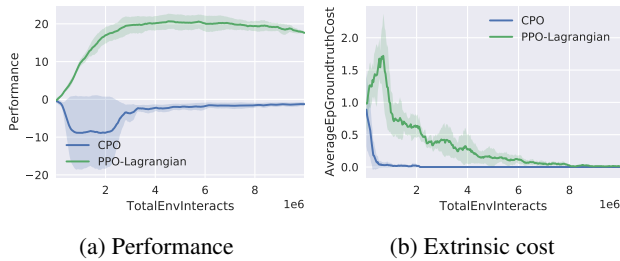


Figure 3: Average episodic reward and cost of safe RL baselines with a dense cost function.

5 Automating Cost Function Design

5.1 Bi-level Optimization Problem

In this paper, we aim to find the intrinsic cost function c_θ^{in} (parameterized by θ) such that the agent π_ω (parameterized by ω) can achieve zero violation by maximizing cumulative

discounted rewards \mathcal{R}^π under the constraint of cost function $c_\theta^{ex+in} = c_\theta^{ex} + c_\theta^{in}$. Formally, our optimization goal is:

$$\begin{aligned} \min_{\theta} \quad & J_{c_\theta^{ex}}^{\pi^*} \\ \text{s.t.} \quad & \pi^* = \arg \max_{\pi \in \Pi_{c_\theta^{ex+in}}} \mathcal{R}^\pi. \end{aligned} \quad (8)$$

Compared with other possible formulations (e.g., considering $J_{c_\theta^{ex+in}}^{\pi^*}$ in the outer loop), the objective in Equation (8) tries to minimize the ground truth constraint violation (i.e., the extrinsic cost objective $J_{c_\theta^{ex}}^{\pi^*}$) to achieve zero violation. This formulation enables safe RL to further eliminate constraint violations. And the corresponding π^* is solved with downstream safe RL algorithms within the feasible policy set $\Pi_{c_\theta^{ex+in}}$ defined by c_θ^{ex+in} .

To find proper cost functions without expert knowledge, we propose AutoCost, a principled solution for resolving the bi-level optimization problem in Equation (8).

5.2 AutoCost

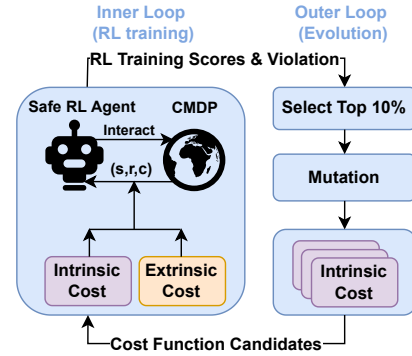


Figure 4: Overview of AutoCost. AutoCost contains an inner loop (left) and an outer loop (right). The inner loop performs an RL training procedure with searched intrinsic cost functions. The outer loop searches intrinsic cost functions using an evolutionary algorithm.

The success of evolution strategies in exploring large, multi-dimensional search space has been proven in many works (Houthoofd et al. 2018; Faust, Francis, and Mehta 2019; Co-Reyes et al. 2020). Similarly, AutoCost adopts an evolutionary algorithm (Bäck and Schwefel 1993) to search for proper cost functions over the parameter space of the intrinsic cost function. The overall pipeline of AutoCost is shown in Figure 4. Specifically, the evolutionary search of AutoCost contains four parts.

- Initialization:** At the beginning of evolutionary search, randomly sample a population of 50 candidates of intrinsic cost functions c_θ^{in} .
- Evaluation:** At each evolution stage, we train RL agents with the population of intrinsic cost functions.
- Selection:** After the inner loop of RL training, all candidates are then sorted by the average episodic extrinsic cost of the converged policy. The top-10% candidates with the lowest constraint violations are selected to generate the population for the next stage. Note that

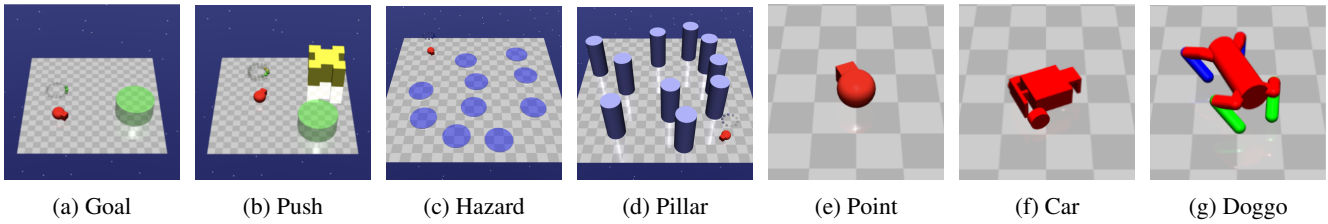


Figure 5: Different tasks, constraints and robots in Safety Gym.

for a population with more than 10% candidates achieving zero violation, we select the top-10% candidates with highest reward performance for the next generation.

4. **Mutation** After selection, we apply mutation on the top intrinsic cost functions to construct the next generation. We design two types of mutations on parameters θ : (i) Gaussian Noise: $\theta' = \theta + z$, where $z \sim \mathcal{N}(0, I)$; (ii) random scaling: $\theta' = \theta * z$, where $z \sim \text{Uni}[\alpha, \beta]$.

6 Experiment

6.1 Environment Setup

We evaluate AutoCost in Safety Gym (Ray, Achiam, and Amodei 2019), a widely used benchmark for safe RL algorithms. Safety Gym is built on an advanced physics engine MuJoCo (Todorov, Erez, and Tassa 2012), with various tasks, constraints and robots. We name these environments as $\{\text{Task}\}-\{\text{Constraint Type}\}-\{\text{Robot}\}$. In our experiments, two tasks are considered:

- **Goal**: The robot must navigate inside the green goal area as shown in Figure 5a.
- **Push**: The robot must push a yellow box inside the green goal area as shown in Figure 5b.

Two different types of constraints are considered:

- **Hazard**: Dangerous (but non-physical) areas as shown in Figure 5c. The agent is penalized for entering them.
- **Pillar**: Fixed obstacles as shown in Figure 5d. The agent is penalized for hitting them.

And three robots are considered:

- **Point**: A simple mobile robot with one actuator for turning and another for moving forward/backwards as shown in Figure 5e.
- **Car**: A wheeled robot with two independently-driven parallel wheels and a free rolling rear wheel as shown in Figure 5f.
- **Doggo**: A quadrupedal robot with bilateral symmetry as shown in Figure 5g. Each of the four legs has two controls at the hip, for azimuth and elevation relative to the torso, and one in the knee, controlling angle.

6.2 Evolution on Safety Gym

Experiment Setting We apply AutoCost to environment Goal-Hazard-Point . To ensure the generalizability of searched intrinsic cost functions to different safe RL algorithms, we train two RL agents (CPO and PPO-Lagrangian) for each intrinsic cost function candidate, and we take

the average episodic extrinsic costs of CPO and PPO-Lagrangian as the evaluation metric. As for the parameter space of the intrinsic cost function, we use a simple multi-layer perception (MLP) neural network with one hidden layer with four neurons, which results in 41 parameters in total including weights and bias. To enforce the intrinsic cost function to be non-negative, we choose the Sigmoid function as the activation function. To further reduce the size of the parameter space, we only include sensors related to constraints (e.g., hazard/pillar lidar) into the input for the intrinsic cost function. Details about input and parameter space of intrinsic cost functions are given in Appendix B.3.

Evolutionary Process The evolution process on the training environment Goal-Hazard-Point is shown in Figure 6. We can observe a clear decreasing trend in the average extrinsic cost of populations as evolution continues, indicating the effectiveness of the evolutionary search. More importantly, the decreasing trend in constraint violation is especially significant in terms of the best intrinsic cost functions in each population. To be more specific, in the population of stage 1, there is no intrinsic cost achieving zero violation. As the population evolves, more and more intrinsic cost functions drive the safe RL algorithms to obtain a zero-violation policy after convergence. Note that the training of each intrinsic cost candidate is parallelizable. More details about computing time can be found in Appendix B.4.

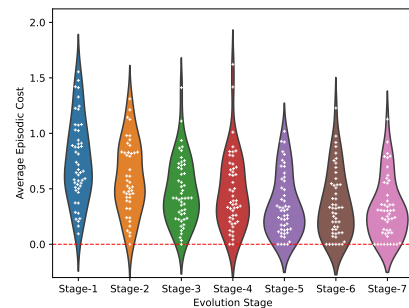
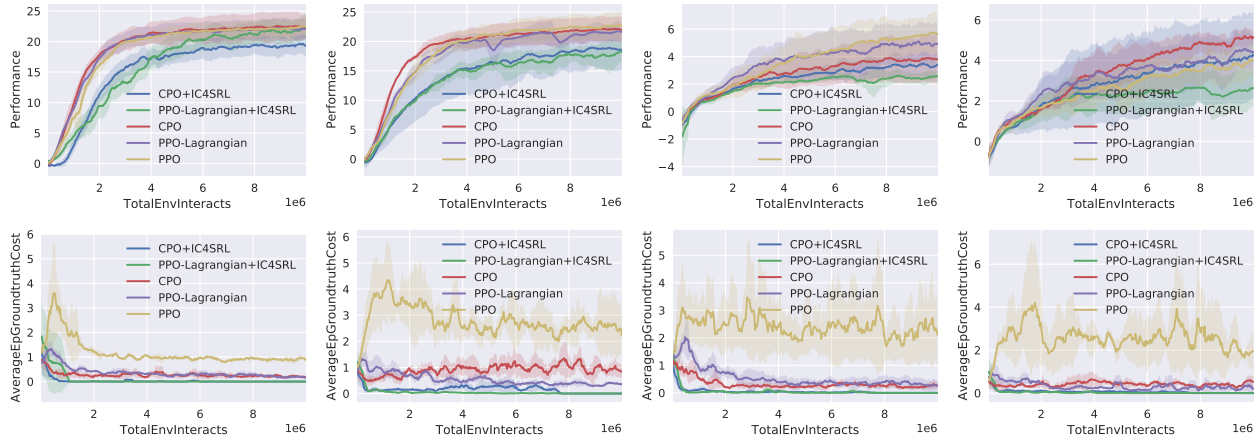


Figure 6: Evolution process in the training environment. Every white dot represents a candidate of the intrinsic cost function, and the y-axis shows its corresponding constraint violations after convergence. The red horizontal line indicates zero-violation safety.

6.3 Generalization Experiments

Among all the intrinsic cost functions achieving zero violation during the evolution, we finalize the candidate with the highest reward performance and name it IC4SRL (intrinsic cost for safe RL). In this section, we further test the generalization ability of IC4SRL in different environments. The



(a) Goal-Hazard-Point (b) Goal-Pillar-Point (c) Push-Hazard-Point (d) Push-Pillar-Point

Figure 7: Average episodic return and extrinsic cost of IC4SRL and baseline methods on Safety Gym Push over five seeds. Goal-Hazard-Point is the training environment of AutoCost while the other three environments are unseen environments for IC4SRL.

methods in the comparison group include: unconstrained RL algorithm **PPO** (Schulman et al. 2017) and constrained safe RL algorithms **PPO-Lagrangian** (Chow et al. 2017), **CPO** (Achiam et al. 2017). We denote **CPO+IC4SRL** and **PPO-Lagrangian+IC4SRL** as the corresponding safe RL methods with IC4SRL as intrinsic cost added to the original extrinsic cost defined in the CMDP. We set the cost limit to zero for all safe RL methods since we aim to avoid any constraint violation. For all experiments, we use the same neural network architectures and hyper-parameter (more details are provided in Appendix B).

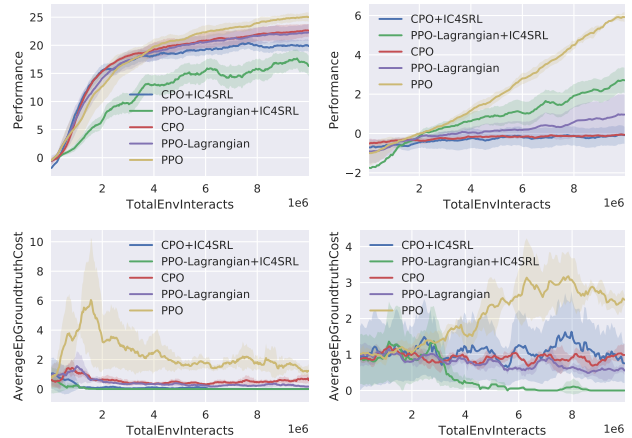
Generalize to Different Tasks and Constraints

IC4SRL is searched from the *training environment* Goal-Hazard-Point, and how well can the intrinsic cost function transfer to different *test environments* remains a question. To answer the question, we first test IC4SRL in different tasks and constraint types. The results are shown in Figure 7, where both CPO+IC4SRL and PPO-Lagrangian+IC4SRL quickly converge to zero-violation policies while CPO and PPO-Lagrangian without intrinsic cost fail to achieve zero violation. The difference between adding intrinsic cost and not adding intrinsic cost proves a proper cost function is a key factor towards achieving zero violation. We also notice that adding intrinsic cost also lowers the reward performance of both CPO and PPO-Lagrangian, indicating the trade-off between safety and performance where IC4SRL drives RL agents to learn more conservative behaviors to avoid any violation.

Generalize to Different Robots

To see whether IC4SRL is able to transfer to different robots, we replace the point robot with more complex robots like car and doggo. The evaluation results are shown in Figure 8. Both CPO+IC4SRL and PPO-Lagrangian+IC4SRL achieve zero violation with the car robot, whereas only PPO-Lagrangian+IC4SRL converges to a zero-violation with the doggo robot. We find that both CPO and CPO+IC4SRL totally fail to gain meaningful rewards in the doggo environment, indicating the zero-violation policy brought by

IC4SRL builds on the precondition that safe RL methods work (i.e., learn meaningful behaviors) in the environment.



(a) Goal-Hazard-Car (b) Goal-Hazard-Doggo

Figure 8: Average episodic return, episodic extrinsic cost of constraints of IC4SRL and baseline methods on Safety Gym with more complex robots over five seeds.

The Limit of Generalization Ability Though IC4SRL successfully generalizes to different environments as shown in Figure 7 and Figure 8, there is still a limit of its generalization ability. One limit is that IC4SRL is only searched with two safe RL algorithms. It is possible that some other safe RL methods require even more conservative intrinsic cost functions to achieve zero violation. Another major limitation is that IC4SRL is coupled with the properties and features of Safety Gym. However, though IC4SRL may be not universal to all settings, one can always apply AutoCost to automatically search for a proper intrinsic cost function for either new safe RL algorithms or new environments.

6.4 Visualization of Intrinsic Cost

To further investigate what the searched intrinsic cost function capture, we visualize IC4SRL in Figure 9a. The blue cir-

cle in the middle represents the hazard. And each grid represents the positions of robots. The results show that IC4SRL assigns intrinsic cost values to the states next to the hazard, indicating that IC4SRL can capture local-aware information about the unsafe state surroundings. This result also echoes recent works (Ma et al. 2021) which adds prior measures to the cost function to improve safety performance. Also the heatmap of intrinsic cost in Figure 9a shows a similar landscape of neural barrier functions (Dawson et al. 2022). But learning a neural barrier function requires pre-defined safe and unsafe regions in the state space, which is hard to design in complex environments. On the contrary, IC4SRL is discovered in a fully automated manner with no expert knowledge required.

To further illustrate why adding intrinsic cost is helpful for achieving zero-violation safe RL policies, we plot the training curve of c_{θ}^{ex+in} in Figure 9b. Note that both safe RL methods fail to lower c_{θ}^{ex+in} under the cost limit of zero. However, the ground truth extrinsic cost quickly converges to zero as shown in Figure 7a. This indicates that adding a more conservative intrinsic cost like IC4SRL is the key to zero violation for safe RL algorithms.

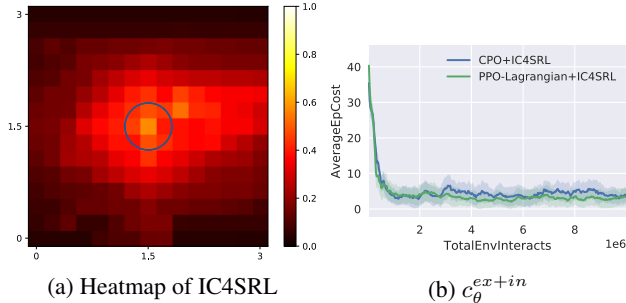


Figure 9: (a) Heatmap of intrinsic cost IC4SRL with different positions of the robot. The blue circle in the middle represents the hazard. (b) The average episodic sum of intrinsic cost and extrinsic cost for CPO+IC4SRL and PPO-Lagrangian+IC4SRL in Goal-Hazard-Point.

6.5 The Necessity of AutoCost

The heatmap shown in Figure 9a demonstrates that intrinsic cost adds an extra margin to the constraint. To justify the necessity of AutoCost, we compare IC4SRL with hand-tuned intrinsic cost with different sizes of the safety margin. The results are shown in Figure 10, where 3x margin and IC4SRL both obtain zero-violation policies after convergence. But IC4SRL achieves much better reward performance, which may be due to the *selection* procedure where AutoCost selects zero-violation candidates with higher reward performance. Note that tuning a proper safety margin (e.g., 3x margin) requires many human efforts while IC4SRL is discovered in a fully automated manner. More importantly, hand-tuned intrinsic cost functions require much prior knowledge (e.g., the size of the constraint and the distances from the robot to the constraint at each time step), which is unrealistic in practice. Nevertheless, AutoCost discovered IC4SRL only with information from lidar sensors, indicating the generalizability of AutoCost to more complex CMDP and black-box safety constraints.

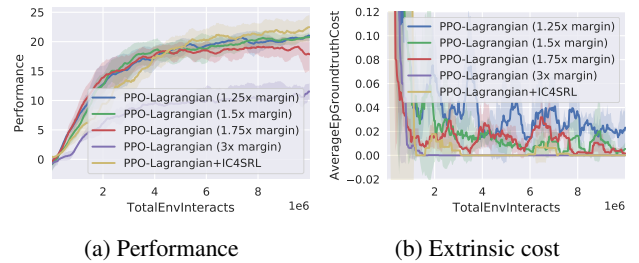


Figure 10: Average episodic return, episodic extrinsic cost of PPO-Lagrangian with hand-tuned intrinsic cost functions with different safety margins.

6.6 With or Without Extrinsic Cost

To test whether safe RL methods are capable of achieving zero violation solely with the intrinsic cost, we denote the safe RL baselines without extrinsic cost function as **CPO+IC4SRL (w/o ex)** and **PPO-Lagrangian+IC4SRL (w/o ex)**. The results are shown in Figure 11. Note that safe RL baselines without extrinsic cost eliminate much more violations compared with baselines using only the extrinsic cost function, which indicates the advantage of IC4SRL over naive indicator cost functions. But both CPO+IC4SRL (w/o ex) and PPO-Lagrangian+IC4SRL (w/o ex) fail to converge to a zero-violation policy. This may be due to the evolutionary process of AutoCost adopting the setting that the cost function is the sum of intrinsic and extrinsic costs and therefore the searched intrinsic cost is limited to that setting.

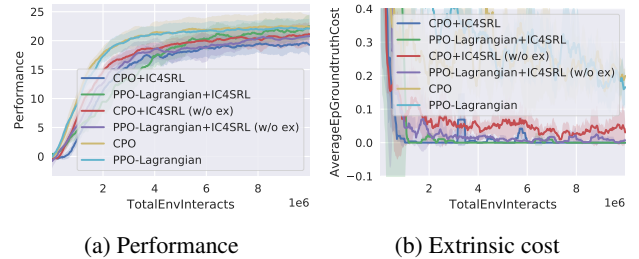


Figure 11: Average episodic return, episodic extrinsic cost of CPO and PPO-Lagrangian with three different cost functions designs: (i) IC4SRL adds intrinsic cost to the extrinsic cost; (ii) IC4SRL (w/o ex) only uses intrinsic cost as the cost function; (iii) vanilla version only uses extrinsic cost.

7 Conclusion

In this paper, we present AutoCost, a principled and universal framework for automated intrinsic cost design for safe RL. This is the first such framework to the best of our knowledge. By searching on Safety Gym with this framework, we discover IC4SRL, a top-performing intrinsic cost function that generalizes well to diverse test environments. Our empirical results show promise in using intrinsic cost function to achieve zero-violation safety performance with safe RL methods like CPO and Lagrangian methods. We hope our studies provide insights that will deepen the understanding of cost function design in safe RL, and shed light on how to enable avenues for real-world deployment of RL in areas like robotics where zero-violation safety is critical.

References

- Achiam, J.; Held, D.; Tamar, A.; and Abbeel, P. 2017. Constrained policy optimization. In *International conference on machine learning*, 22–31. PMLR.
- Ahmadi, A. A.; and Majumdar, A. 2016. Some applications of polynomial optimization in operations research and real-time decision making. *Optimization Letters*, 10(4): 709–729.
- Altman, E. 1999. *Constrained Markov decision processes: stochastic modeling*. Routledge.
- Ames, A. D.; Grizzle, J. W.; and Tabuada, P. 2014. Control barrier function based quadratic programs with application to adaptive cruise control. In *53rd IEEE Conference on Decision and Control*, 6271–6278. IEEE.
- Andrychowicz, M.; Wolski, F.; Ray, A.; Schneider, J.; Fong, R.; Welinder, P.; McGrew, B.; Tobin, J.; Pieter Abbeel, O.; and Zaremba, W. 2017. Hindsight experience replay. *Advances in neural information processing systems*, 30.
- Bäck, T.; and Schwefel, H.-P. 1993. An overview of evolutionary algorithms for parameter optimization. *Evolutionary computation*, 1(1): 1–23.
- Berkenkamp, F.; Turchetta, M.; Schoellig, A.; and Krause, A. 2017. Safe model-based reinforcement learning with stability guarantees. *Advances in neural information processing systems*, 30.
- Bharadhwaj, H.; Kumar, A.; Rhinehart, N.; Levine, S.; Shkurti, F.; and Garg, A. 2020. Conservative safety critics for exploration. *arXiv preprint arXiv:2010.14497*.
- Boyd, S.; Boyd, S. P.; and Vandenberghe, L. 2004. *Convex optimization*. Cambridge university press.
- Brown, N.; and Sandholm, T. 2018. Superhuman AI for heads-up no-limit poker: Libratus beats top professionals. *Science*, 359(6374): 418–424.
- Chang, Y.-C.; Roohi, N.; and Gao, S. 2019. Neural lyapunov control. *Advances in neural information processing systems*, 32.
- Chen, Y.; Dong, J.; and Wang, Z. 2021. A primal-dual approach to constrained markov decision processes. *arXiv preprint arXiv:2101.10895*.
- Chow, Y.; Ghavamzadeh, M.; Janson, L.; and Pavone, M. 2017. Risk-constrained reinforcement learning with percentile risk criteria. *The Journal of Machine Learning Research*, 18(1): 6070–6120.
- Chow, Y.; Nachum, O.; Duenez-Guzman, E.; and Ghavamzadeh, M. 2018. A lyapunov-based approach to safe reinforcement learning. *Advances in neural information processing systems*, 31.
- Co-Reyes, J. D.; Miao, Y.; Peng, D.; Real, E.; Le, Q. V.; Levine, S.; Lee, H.; and Faust, A. 2020. Evolving Reinforcement Learning Algorithms. In *International Conference on Learning Representations*.
- Dalal, G.; Dvijotham, K.; Vecerik, M.; Hester, T.; Paduraru, C.; and Tassa, Y. 2018. Safe exploration in continuous action spaces. *arXiv preprint arXiv:1801.08757*.
- Dawson, C.; Gao, S.; and Fan, C. 2022. Safe Control with Learned Certificates: A Survey of Neural Lyapunov, Barrier, and Contraction methods. *arXiv preprint arXiv:2202.11762*.
- Dawson, C.; Qin, Z.; Gao, S.; and Fan, C. 2022. Safe nonlinear control using robust neural lyapunov-barrier functions. In *Conference on Robot Learning*, 1724–1735. PMLR.
- Dewey, D. 2014. Reinforcement learning and the reward engineering principle. In *2014 AAAI Spring Symposium Series*.
- El Chamie, M.; Yu, Y.; and Açıkmeşe, B. 2016. Convex synthesis of randomized policies for controlled Markov chains with density safety upper bound constraints. In *2016 American Control Conference (ACC)*, 6290–6295. IEEE.
- Faust, A.; Francis, A.; and Mehta, D. 2019. Evolving rewards to automate reinforcement learning. *arXiv preprint arXiv:1905.07628*.
- Ferlez, J.; Elnaggar, M.; Shoukry, Y.; and Fleming, C. 2020. Shieldnn: A provably safe nn filter for unsafe nn controllers. *CoRR*, abs/2006.09564.
- Franke, J. K.; Köhler, G.; Biedenkapp, A.; and Hutter, F. 2020. Sample-efficient automated deep reinforcement learning. *arXiv preprint arXiv:2009.01555*.
- Giesl, P.; and Hafstein, S. 2015. Review on computational methods for Lyapunov functions. *Discrete & Continuous Dynamical Systems-B*, 20(8): 2291.
- Gracia, L.; Garelli, F.; and Sala, A. 2013. Reactive sliding-mode algorithm for collision avoidance in robotic systems. *IEEE Transactions on Control Systems Technology*, 21(6): 2391–2399.
- Hong, Z.-W.; Shann, T.-Y.; Su, S.-Y.; Chang, Y.-H.; Fu, T.-J.; and Lee, C.-Y. 2018. Diversity-driven exploration strategy for deep reinforcement learning. *Advances in neural information processing systems*, 31.
- Houthoofd, R.; Chen, Y.; Isola, P.; Stadie, B.; Wolski, F.; Jonathan Ho, O.; and Abbeel, P. 2018. Evolved policy gradients. *Advances in Neural Information Processing Systems*, 31.
- Khatib, O. 1986. Real-time obstacle avoidance for manipulators and mobile robots. In *Autonomous robot vehicles*, 396–404. Springer.
- Kong, J.; Pfeiffer, M.; Schildbach, G.; and Borrelli, F. 2015. Kinematic and dynamic vehicle models for autonomous driving control design. In *2015 IEEE Intelligent Vehicles Symposium (IV)*, 1094–1099. IEEE.
- Liang, Q.; Que, F.; and Modiano, E. 2018. Accelerated primal-dual policy optimization for safe reinforcement learning. *arXiv preprint arXiv:1802.06480*.
- Liu, C.; and Tomizuka, M. 2014. Control in a safe set: Addressing safety in human-robot interactions. In *Dynamic Systems and Control Conference*, volume 46209, V003T42A003. American Society of Mechanical Engineers.
- Ma, H.; Liu, C.; Li, S. E.; Zheng, S.; Sun, W.; and Chen, J. 2021. Learn Zero-Constraint-Violation Policy in Model-Free Constrained Reinforcement Learning. *arXiv preprint arXiv:2111.12953*.

- Mnih, V.; Kavukcuoglu, K.; Silver, D.; Rusu, A. A.; Veness, J.; Bellemare, M. G.; Graves, A.; Riedmiller, M.; Fidjeland, A. K.; Ostrovski, G.; et al. 2015. Human-level control through deep reinforcement learning. *nature*, 518(7540): 529–533.
- Paul, S.; Kurin, V.; and Whiteson, S. 2019. Fast efficient hyperparameter tuning for policy gradient methods. *Advances in Neural Information Processing Systems*, 32.
- Qin, Z.; Zhang, K.; Chen, Y.; Chen, J.; and Fan, C. 2021. Learning safe multi-agent control with decentralized neural barrier certificates. *arXiv preprint arXiv:2101.05436*.
- Ray, A.; Achiam, J.; and Amodei, D. 2019. Benchmarking safe exploration in deep reinforcement learning. *CoRR*, abs/1910.01708.
- Runge, F.; Stoll, D.; Falkner, S.; and Hutter, F. 2018. Learning to design RNA. *arXiv preprint arXiv:1812.11951*.
- Schulman, J.; Levine, S.; Abbeel, P.; Jordan, M.; and Moritz, P. 2015. Trust region policy optimization. In *International conference on machine learning*, 1889–1897. PMLR.
- Schulman, J.; Wolski, F.; Dhariwal, P.; Radford, A.; and Klimov, O. 2017. Proximal Policy Optimization Algorithms. *CoRR*, abs/1707.06347.
- Srinivasan, K.; Eysenbach, B.; Ha, S.; Tan, J.; and Finn, C. 2020. Learning to be safe: Deep rl with a safety critic. *arXiv preprint arXiv:2010.14603*.
- Stooke, A.; Achiam, J.; and Abbeel, P. 2020. Responsive safety in reinforcement learning by pid lagrangian methods. In *International Conference on Machine Learning*, 9133–9143. PMLR.
- Tessler, C.; Mankowitz, D. J.; and Mannor, S. 2018. Reward constrained policy optimization. *arXiv preprint arXiv:1805.11074*.
- Todorov, E.; Erez, T.; and Tassa, Y. 2012. Mujoco: A physics engine for model-based control. In *2012 IEEE/RSJ international conference on intelligent robots and systems*, 5026–5033. IEEE.
- Veeriah, V.; Hessel, M.; Xu, Z.; Rajendran, J.; Lewis, R. L.; Oh, J.; van Hasselt, H. P.; Silver, D.; and Singh, S. 2019. Discovery of useful questions as auxiliary tasks. *Advances in Neural Information Processing Systems*, 32.
- Vinyals, O.; Babuschkin, I.; Czarnecki, W. M.; Mathieu, M.; Dudzik, A.; Chung, J.; Choi, D. H.; Powell, R.; Ewalds, T.; Georgiev, P.; et al. 2019. Grandmaster level in StarCraft II using multi-agent reinforcement learning. *Nature*, 575(7782): 350–354.
- Wei, T.; and Liu, C. 2019. Safe control algorithms using energy functions: A unified framework, benchmark, and new directions. In *2019 IEEE 58th Conference on Decision and Control (CDC)*, 238–243. IEEE.
- Xu, Z.; van Hasselt, H. P.; Hessel, M.; Oh, J.; Singh, S.; and Silver, D. 2020. Meta-gradient reinforcement learning with an objective discovered online. *Advances in Neural Information Processing Systems*, 33: 15254–15264.
- Zahavy, T.; Xu, Z.; Veeriah, V.; Hessel, M.; Oh, J.; van Hasselt, H. P.; Silver, D.; and Singh, S. 2020. A self-tuning actor-critic algorithm. *Advances in Neural Information Processing Systems*, 33: 20913–20924.
- Zhang, Y.; Vuong, Q.; and Ross, K. 2020. First order constrained optimization in policy space. *Advances in Neural Information Processing Systems*, 33: 15338–15349.
- Zhao, W.; He, T.; and Liu, C. 2021. Model-free safe control for zero-violation reinforcement learning. In *5th Annual Conference on Robot Learning*.
- Zheng, Z.; Oh, J.; and Singh, S. 2018. On learning intrinsic rewards for policy gradient methods. *Advances in Neural Information Processing Systems*, 31.

A More Experiment Results

A.1 More Hand-deigned Cost Functions

In this subsection, we present more experiment results of several other hand-designed cost functions to illustrate the difficulty of manually designing cost functions.

Distance Change We design a cost function based on the change of distance between two time steps:

$$c(s_t) = d(s_{t-1}) - d(s_t), \quad (9)$$

where $d(\cdot)$ denotes the distance from RL agent to the closet constraint. Note that the difference between Equation (9) and Equation (7) is whether to enforce the cost function to be non-negative. We train CPO and PPO-Lagrangian under the denser cost function. The results are shown in Figure 12, where both CPO and PPO-Lagrangian fail to lower the average episodic extrinsic cost to zero. The main reason for such failure is that the cost function defined in Equation (9) could be negative, which make the zero cost limit invalid for most scenarios. This result proves the necessity of a non-negative cost function.

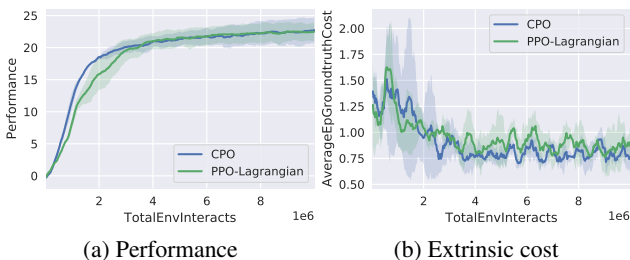


Figure 12: Average episodic reward and cost of safe RL baselines with a cost function based on the change of distance.

Indicator Distance Change We design a cost function based on the change of distance between two time steps:

$$c(s_t) = \mathbb{1}[d(s_{t-1}) - d(s_t) \geq 0], \quad (10)$$

where $d(\cdot)$ denotes the distance from RL agent to the closet constraint. Note the cost function assigns 1 to any step getting closer to the constraint and 0 otherwise. We train CPO and PPO-Lagrangian under the cost function defined in Equation (10). The results are shown in Figure 13, where both CPO converges to a zero-violation policy while PPO-Lagrangian obtains a near zero-violation policy after convergence. But both CPO and PPO-Lagrangian suffer from terrible reward performance drop.

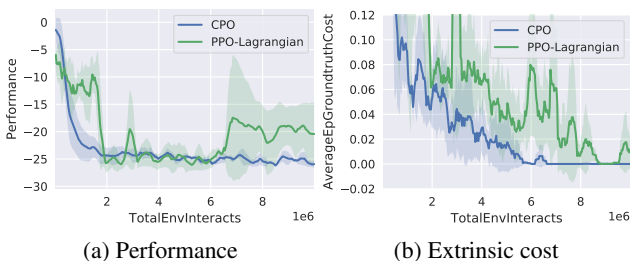


Figure 13: Average episodic reward and cost of safe RL baselines with a cost function based on the change of distance.

A.2 CPO with Different Safety Margins

To justify the necessity of AutoCost, we compare IC4SRL with hand-tuned intrinsic cost with different sizes of the safety margin. As shown in Figure 14, the results of CPO are similar to PPO-Lagrangian, where 3x margin and IC4SRL both obtain zero-violation policies after convergence. But IC4SRL achieves much better reward performance than CPO (3x margin).

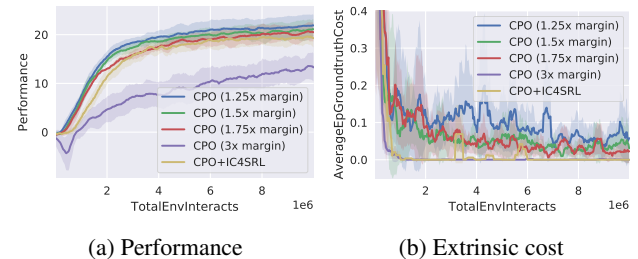


Figure 14: Average episodic return, episodic extrinsic cost of PPO-Lagrangian with hand-tuned intrinsic cost functions with different safety margins.

B Experiment Details

B.1 Environment Settings

Goal Task In the Goal task environments, the reward function is:

$$r(x_t) = d_{t-1}^g - d_t^g + \mathbb{1}[d_t^g < R^g],$$

where d_t^g is the distance from the robot to its closest goal and R^g is the size (radius) of the goal. When a goal is achieved, the goal location is randomly reset to someplace new while keeping the rest of the layout the same.

Push Task In the Push task environments, the reward function is:

$$r(x_t) = d_{t-1}^r - d_t^r + d_{t-1}^b - d_t^b + \mathbb{1}[d_t^b < R^g],$$

where d_t^r and d_t^b are the distance from the robot to its closest goal and the distance from the box to its closest goal, and R^g is the size (radius) of the goal. The box size is 0.2 for all the Push task environments. Like the goal task, a new goal location is drawn each time a goal is achieved.

Hazard Constraint In the Hazard constraint environments, the cost function is:

$$c(x_t) = \max(0, R^h - d_t^h),$$

where d_t^h is the distance to the closest hazard and R^h is the size (radius) of the hazard.

Pillar Constraint In the Pillar constraint environments, the cost $c_t = 1$ if the robot contacts with the pillar otherwise $c_t = 0$.

State Space The state space is composed of various physical quantities from standard robot sensors (accelerometer, gyroscope, magnetometer, and velocimeter) and lidar (where each lidar sensor perceives objects of a single kind). The state spaces of all the test suites are summarized in Table 1.

Table 1: The state space components of different test suites environments.

| State Space Option | Goal-Hazard | Goal-Pillar | Push-Hazard | Push-Pillar |
|--------------------|-------------|-------------|-------------|-------------|
| Accelerometer | ✓ | ✓ | ✓ | ✓ |
| Gyroscope | ✓ | ✓ | ✓ | ✓ |
| Magnetometer | ✓ | ✓ | ✓ | ✓ |
| Velocimeter | ✓ | ✓ | ✓ | ✓ |
| Goal Lidar | ✓ | ✓ | ✓ | ✓ |
| Hazard Lidar | ✓ | ✗ | ✓ | ✗ |
| Pillar Lidar | ✗ | ✓ | ✗ | ✓ |
| Box Lidar | ✗ | ✗ | ✓ | ✓ |

B.2 Policy Settings

Detailed parameter settings are shown in Table 2. All the policies in our experiments use the default hyper-parameter settings hand-tuned by Safety Gym (Berkenkamp et al. 2017).

B.3 Intrinsic Cost Settings

As introduced in Table 1, there are many components of the state space while some of the components are irrelevant to cost functions designs (e.g. lidar information of goal). Therefore, we only select cost-relevant information (i.e., lidar information of hazard/pillar) as the input features for the intrinsic cost function. The parameter space of the intrinsic cost function is the parameter space of the 1-hidden-layer (with four neurons) MLP we used. The input features of lidar information of constants are 8-dimensional. Together with the MLP (five hidden neurons and one output scale neuron), we have 41 parameters in total for the MLP of intrinsic cost functions including weights and bias.

B.4 Computing Infrastructure

We present the computing infrastructure and the corresponding computational time used in Table 3 and Table 4. During the evolution, note that the training of each intrinsic cost candidate can be parallel. With sufficient computing power, the computing time of AutoCost only scales linearly with stages. Due to the limitation of our computing infrastructure, we can only make half of the training of one population (25 candidates / 50 candidates) parallel. The corresponding computing time is shown in Table 4.

| | |
|--------|-----------------------------|
| CPU | AMD 3970X 32-Core Processor |
| GPU | RTX2080TIx2 |
| Memory | 256GB |

Table 3: The computing infrastructure.

| Tasks | Computation time in hours |
|-------------------------------|---------------------------|
| Goal-Hazard-Point | 3.8 |
| Goal-Hazard-Pillar | 3.7 |
| Push-Hazard-Point | 4.4 |
| Push-Hazard-Pillar | 4.2 |
| Goal-Hazard-Car | 4.1 |
| Goal-Hazard-Doggo | 4.2 |
| Goal-Hazard-Point (evolution) | 54.1 |

Table 4: The computing infrastructure.

| Policy Parameter | PPO | PPO-Lagrangian & PPO-Lagrangian+IC4SRL | CPO & CPO+IC4SRL |
|---------------------------------------|------------|--|------------------|
| Timesteps per iteration | 30000 | 30000 | 30000 |
| Policy network hidden layers | (256, 256) | (256, 256) | (256, 256) |
| Value network hidden layers | (256, 256) | (256, 256) | (256, 256) |
| Policy learning rate | 0.0004 | 0.0004 | (N/A) |
| Value learning rate | 0.001 | 0.001 | 0.001 |
| Target KL | 0.01 | 0.01 | 0.01 |
| Discounted factor γ | 0.99 | 0.99 | 0.99 |
| Advantage discounted factor λ | 0.97 | 0.97 | 0.97 |
| PPO Clipping ϵ | 0.2 | 0.2 | (N/A) |
| TRPO Conjugate gradient damping | (N/A) | (N/A) | 0.1 |
| TRPO Backtracking steps | (N/A) | (N/A) | 10 |
| Cost limit | (N/A) | 0 | 0 |

Table 2: Important hyper-parameters of PPO, PPO-Lagrangian, CPO. Note that all the hyper-parameters are fixed the same across different environments with or without intrinsic cost functions.